

## **Chapter 10: Application of Wavelet Transforms to Structural Damage Monitoring and Detection**

### **Chapter details**

**Chapter DOI:**

<https://doi.org/10.4322/978-65-86503-71-5.c10>

**Chapter suggested citation / reference style:**

Palechor, Erwin U. L., et al. (2022). “Application of Wavelet Transforms to Structural Damage Monitoring and Detection”. In Jorge, Ariosto B., et al. (Eds.) *Model-Based and Signal-Based Inverse Methods*, Vol. I, UnB, Brasilia, DF, Brazil, pp. 357–381. Book series in Discrete Models, Inverse Methods, & Uncertainty Modeling in Structural Integrity.

**P.S.:** DOI may be included at the end of citation, for completeness.

### **Book details**

**Book:** Model-based and Signal-Based Inverse Methods

**Edited by:** Jorge, Ariosto B., Anflor, Carla T. M., Gomes, Guilherme F., & Carneiro, Sergio H. S.

**Volume I of Book Series in:**

Discrete Models, Inverse Methods, & Uncertainty Modeling in Structural Integrity

**Published by:** UnB City: Brasilia, DF, Brazil Year: 2022

**DOI:** <https://doi.org/10.4322/978-65-86503-71-5>

# Application of Wavelet Transforms to Structural Damage Monitoring and Detection

Erwin Ulises Lopez Palechor<sup>1\*</sup>, Ramon Saleno Yure Costa Silva<sup>2</sup>, Gilberto Gomes<sup>2</sup>, Marcus V. Girão de Moraes<sup>2,4</sup>, Luciano Mendes Bezerra<sup>3</sup> and Ariosto Bretanha Jorge<sup>4</sup>

<sup>1</sup> Science and Technology Center, Federal University of Cariri, Brazil. e-mail: erwin.lopez@ufca.edu.br

<sup>2</sup> Faculty of Technology, University of Brasilia, Brazil. e-mail: ggomes@unb.br; ramon.silva@unb.br; mvmorais@unb.br

<sup>3</sup> Post-Graduate Program in Structures and Civil Construction, University of Brasilia, Brazil. e-mail: lmbz@unb.br

<sup>4</sup> Post-Graduate Program in Integrity of Engineering Materials, University of Brasilia, Brazil. e-mail: ariosto.b.jorge@gmail.com

\*Corresponding author

## *Abstract*

*This chapter presents applications of Wavelet Transforms in damage identification, in 1D 2D and 3D structures, using numerical and experimental data, the research works developed at the Graduate Program of Structures and Civil Construction of University of Brasilia.*

**Keywords:** Wavelet application, Structural Health Monitoring, Wavelet Transform, Continuous Wavelet, Discrete Wavelet, Wavelet Family Function.

## **1 Wavelet Applications Review on Damage Detection of Structures**

Damage detection and localization inside structures has great importance due to being critical for the serviceability and safety of structural elements. Only ultrasonic and x-ray are reliable techniques for nondestructive examination of structures. They may be applied in practice for the precise location of subsurface damages. Both of them require special procedures and are time consuming and expensive. Current research point toward the possible use of numerical-computational methods in assisting the detection of damages inside structures.

Vibration-based methods of damage detection rely on the fact that dynamic characteristics such as natural frequencies, mode shapes and damping are influenced by stiffness (Friswell, 2007; Janeliukstis *et al.*, 2017). The most serious limitation of those methods is the need for a structural response of the healthy structure. But, in the past few years, wavelet transform analysis have attracted attention for vibration-based damage localization techniques (Kim and Melhem, 2004; Yang and Oyadiji, 2017). The wavelet transform analysis has the advantage of need only damage structure response.

Palechor (2013) presents experimental results using Wavelet Transform to determine the damage localization in a laminated steel beam (I-profile), using the static response (displacements) of the damaged beam.

Silva, Palechor et al. (2019) presents a damage localization analysis using experimental data of Dogna Bridge, Italy. In this case, this methodology use CWT of experimental modal shape, with cubic spline interpolation and regularization techniques, to localize damage in beam grid structures. The paper uses experimental results and calibrate numerical model to localize induced damage. The experimental/numerical methodology do not need comparison to intact structural model.

Silva, Bezerra et al (2019) associate boundary element method with wavelet transform to detect and localize damage in structures subjected to static loads. The applications cases concern the localization of subsurface cracks in structures two-dimensional with different support conditions. This methodology investigates two-dimensional structures with single and multiple cracks with different orientations inside. The effectiveness of this methodology is discussed through the resumé of principal numerical results obtained.

All presented applications of damage localization using Wavelet Transforms, in 1D 2D and 3D structures, are research results developed by Graduate Program of Structures and Civil Construction of University of Brasília.

## 2 Basics Concepts of Wavelet Transform

The Wavelet Transform, widely used in several engineering domain, was applied to damage detection in structures. Damage is a local phenomenon is not sensible apparent in vibration response data of structure. Wavelet transform can identify even slight changes in global response of vibrational signal. Wavelet transform make possible this using base functions  $\psi(x)$ , called wavelets, to analysis any signal in several scale and position (Palechor *et al.*, 2022). Wavelet Transform projects a signal into two-dimensional space, function of scale and position.

The Continuous Wavelet Transform (CWT) of the signal  $f(x)$  is defined as:

$$W_{\psi}^f(a, b) = \int_{-\infty}^{\infty} f(x)\psi_{a,b}(x)dx \quad (1)$$

where,  $\psi_{a,b}(x) = |a|^{-1/2}\psi'(x - b/a)$  is the mother wavelet function, and coefficients  $a$  and  $b$  are scale and position, respectively.

The Discrete Wavelet Transform (DWT) (Ovanesova, 2000; Ovanesova and Suárez, 2004; Palechor *et al.*, 2022) of the signal  $f(x)$  is defined as:

$$W_{j,k} = \int_{-\infty}^{\infty} f(x)\psi_{j,k}(x)dx \quad (2)$$

where,  $\psi_{j,k}(x) = \psi(2^{-j}x - k)$  is the discrete mother wavelet; the scale  $a = 2^j$  and the shifting  $b = k(2^j)$ , where  $(j, k) \in Z$  (integer set).

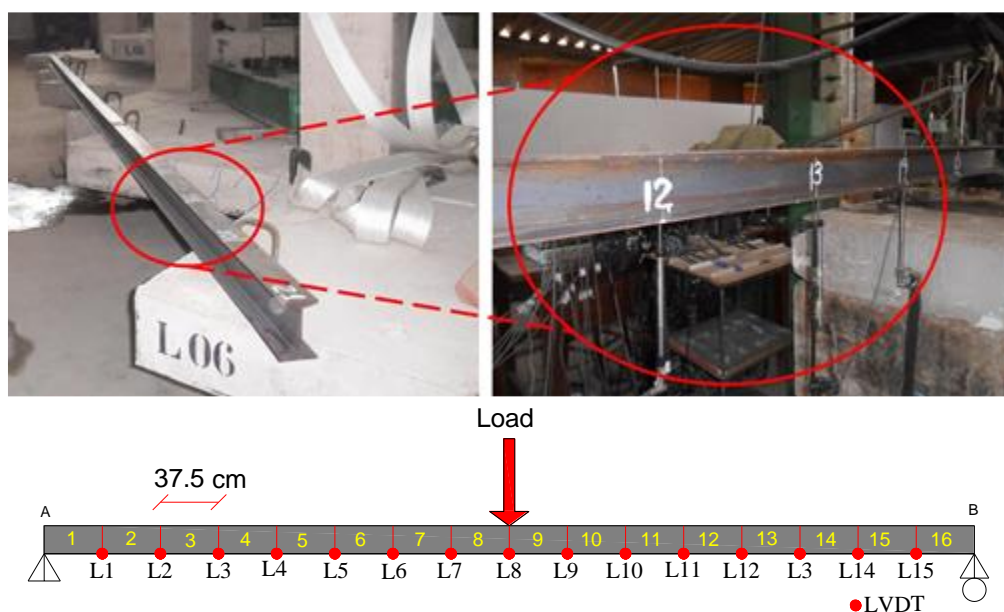
The wavelet coefficients  $W_{\psi}^f(a, b)$  (for CWT) and  $W_{j,k}$  (for DWT) has a property to be sensitive to local singularities in signal. This property is particularly useful to identify a beam discontinuity due to a loss of stiffness (stiffness damage).

### 3 Damage Detection of Steel Beams using Static Displacement

Using experimental results, Wavelet transform is applied to figure out the open crack position in damage laminated steel beam.

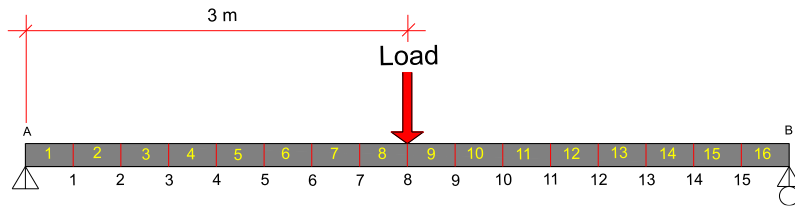
The metallic beams evaluated is simply supported beam in MR-250 steel, with 6m of length, subjected to various levels of load applied at middle-span. The geometric and material characteristics of essayed beams are shown in Table 1. It is worth mentioning that the values, the yield stress ( $f_y$ ), modulus of elasticity (E) and Poisson's ratio ( $\nu$ ), were chosen from the catalog provided by the manufacturer.

Figure 1 show the discretization of beams span into sixteen longitudinal segments, with a length  $\Delta L = 375\text{mm}$ , totaling 17 nodal points.



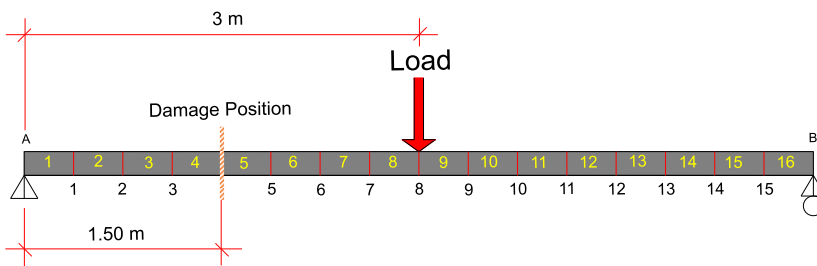
**Figure 1 – Schematic representation of steel beam discretization into 16 segments.**

Figure 2 show schematic representation for location and characteristics of induced damage on essayed beams. The load application in mid-span was the same for all essays, at node 8.



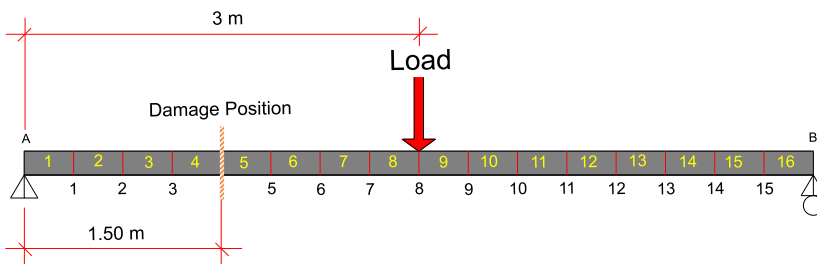
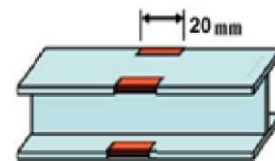
(a) Intact Beam V1E

INTACT BEAM V1E  
- intact beam with load applied at mid-span.



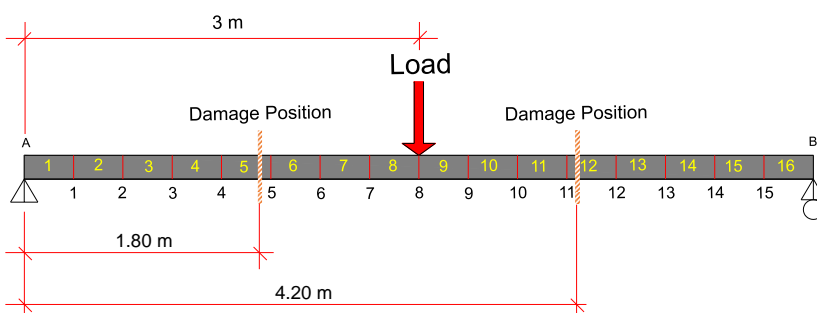
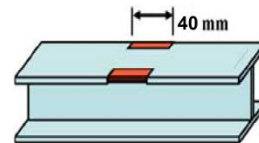
(b) Damage Beam V2E.

DAMAGE BEAM V2E  
- damage location at 1.50m of left support  
- damage length of 2 cm.



(c) Damage Beam V2E-2.

DAMAGE BEAM V2E-2  
- damage location at 1.50m of left support  
- damage length of 4 cm.



DAMAGE BEAM V3  
- damage location at 1.50m and 4.2m of left support  
- damage length of 2cm.

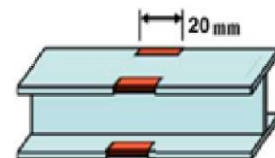


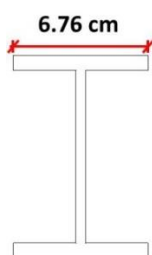
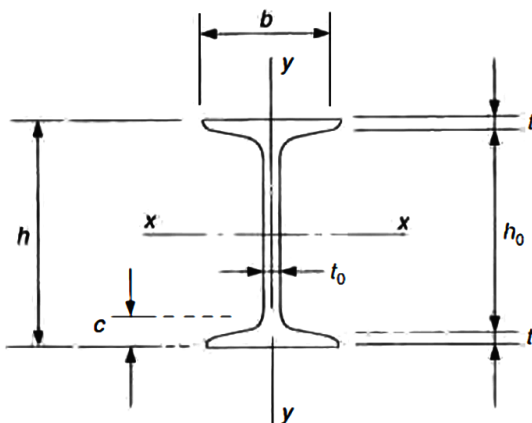
Figure 2 – Schematic description of induced damage for each experimental static essays

The induced damage was carried out using a circular saw with cuts with 2cm or 4cm length in longitudinal direction. Both open cracks induce a decrease of second moment of in cross section (Figure 3).

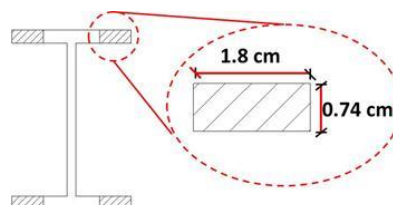
Table 2 shows area moment of inertia for intact and damage section.

**Table 1 – Material and geometric characteristics of essayed beam.**

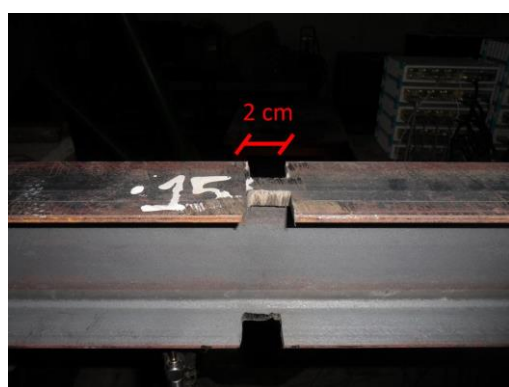
Steel I-shape 102 X 11,4	
h(cm)	10,16
h <sub>0</sub> (cm)	8,68
t <sub>f</sub> (cm)	0,74
t <sub>0</sub> (cm)	0,483
c(cm)	1,59
b(cm)	6,76
Surface (cm <sup>2</sup> )	14,5
I <sub>x</sub> (cm <sup>4</sup> )	252
W <sub>x</sub> (cm <sup>3</sup> )	49,7
i <sub>x</sub> (cm)	4,17
I <sub>y</sub> (cm <sup>4</sup> )	31,7
W <sub>y</sub> (cm <sup>3</sup> )	9,37
i <sub>y</sub> (cm)	1,48
Z <sub>x</sub> (cm <sup>3</sup> )	56,220
Z <sub>y</sub> (cm <sup>3</sup> )	17,414
f <sub>y</sub> (kN/cm <sup>2</sup> )	25
E (kN/cm <sup>2</sup> )	20000
Length L (m)	6



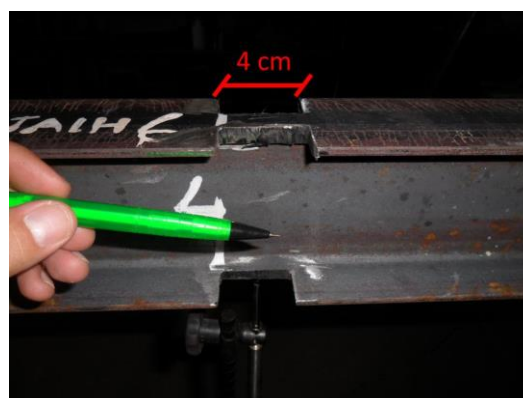
(a) intact beam



(b) transversal section of damage



(c) 2cm induced damage



(d) 4cm induced damage

**Figure 3 – Geometry of induced damage in steel beam**

**Table 2 – Decreased moment of inertia of the cross section induced by open crack**

	$I_x (cm^4)$	$I_y (cm^4)$	$r_x^1 (cm)$	$r_y (cm)$
<b>Intact Section</b>	252	31,7	4,17	1,48
<b>Damage Section</b>	130,71	4,0215	3,83	0,67

To ensure simple support (Figure 4a), two plane plates and a roller were used to allow displacement only in the x direction. For the hinged support (Figure 4b), two grooved plates with a roller were designed to restrict the translation in all direction, permitting only rotation.

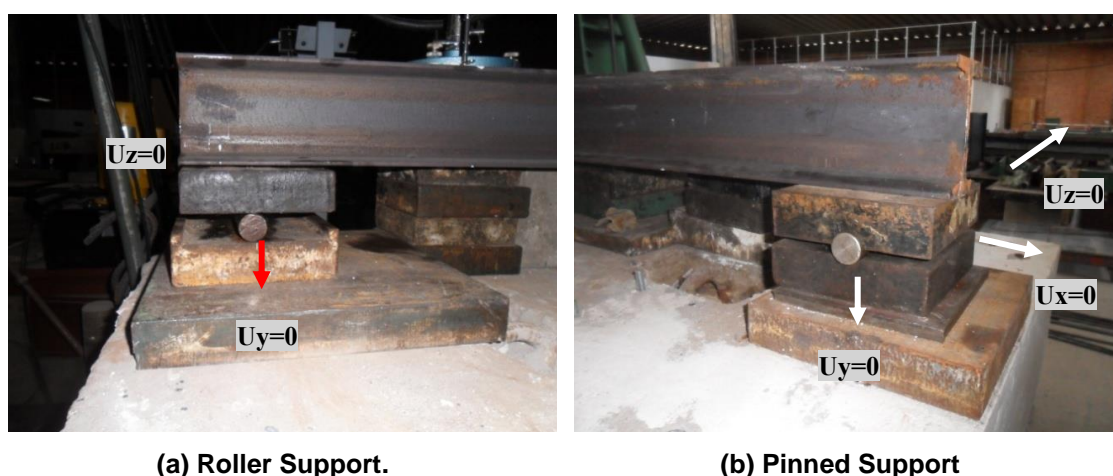


**Figure 4 – Structural support description of steel span.**

Along of steel beam, seventeen LVDTs collected the experimental data corresponding to nodal vertical displacements for essayed beams. Exported to Matlab, experimental data was interpolated, using cubic-spline tool (`spline` command), to smooth data with more registers. The Tikhonov regularization method was applied to the interpolation results. As a last procedure, the damage identification was done using TDW and TCW.

For each essayed beam, Table 3 describe the correspondence of damage location for spatial position and wavelet node (signal position) to make easy the visualization of wavelet coefficients.

**Table 3 – Correspondence between spatial distance and wavelet node to each damage beam.**

<b>Beam</b>	<b>Position(m) from left support</b>	<b>Node (#) TDW</b>	<b>Node (#) TCW</b>
V2E	damage of 2cm at 1,5 m	25	250
V2E-2	damage of 4cm at 1,5 m	25	250
V3E	damage of 2cm at 1,8 m and 4,2 m	30 e 70	300 e 700

<sup>1</sup> Radius of gyration  $r = \sqrt{I/A}$  ( $r_x, r_y$ )

Figure 5 show experimental results of vertical displacements  $U_y$  for each tested beam statically essayed. Each steel beam is subjected for several static load levels. But wavelet transform was obtained for an intermediated load (V2E – 3330N, V2E-2 – 3990N and V3E – 3120N), inferior of maximum resistance load of intact beam (4373N).

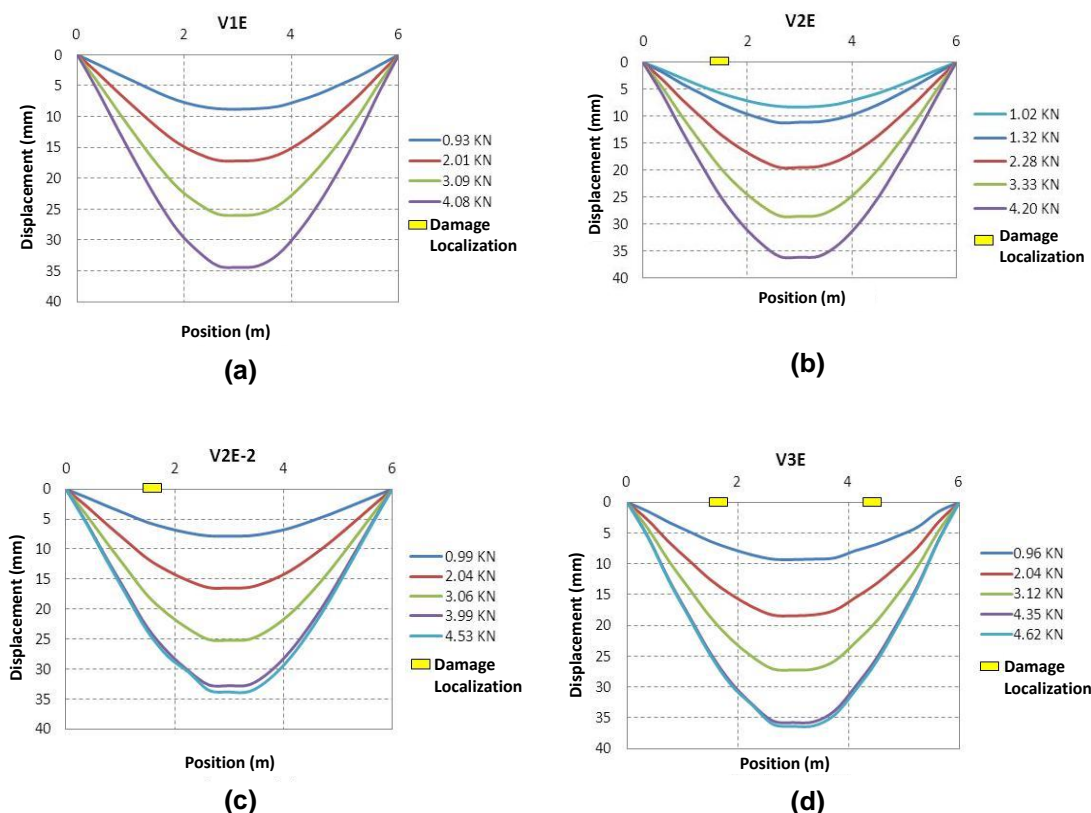


**Figure 5 – Horizontal displacement of structural span for study conditions: (a) intact beam, and damage beam V2E (b), V2E-2 (c) and V3E (d).**

The damage location was performed using only the static experimental responses of damaged beams V2E, V2E-2 and V3E. The obtained results with DWT and CWT are presented below.

### 3.1 Discrete wavelet transform results

From all mother wavelet functions in Matlab to calculate TDW coefficients, Palechor et al. (2014) analyses four mother wavelets (bior6.8, rbio2.6, sym6, coif3 and db5). For this chapter, Daubechies mother wavelet (db5) are presents due the fact of others mother wavelets analyzed is similar.

Figure 6 show discrete wavelets coefficients of experimental static data of V2E beam using Daubechies mother wavelet (db5). The damage is located at node 25 corresponding to 1.5 m from left support. At node 25, the DWT coefficients observe a small peak around the damaged region surrounding by others smaller ones due to signal noise. In addition,



DWT generated disturbances at the extremity of DWT coefficient data, due to the geometric discontinuities of the supports.

Figure 7 show discrete wavelets coefficients of experimental static data of V2E-E beam with damage location at node 25. Compared to V2E (Figure 6), the DWT coefficients observe a highest pick due to the increase of open crack, now with 4cm. The noise pollution surrounding the damage is smaller too.

The V3E beam have two open cracks located at node 30 (1.8m from left support) and at node 70 (4.2 m). Figure 8 show discrete wavelets coefficients of experimental static data of V3E-E beam. The discrete wavelets coefficients were able to detect clearly the open crack at 70. The damage locates at node 30 have smaller spikes.

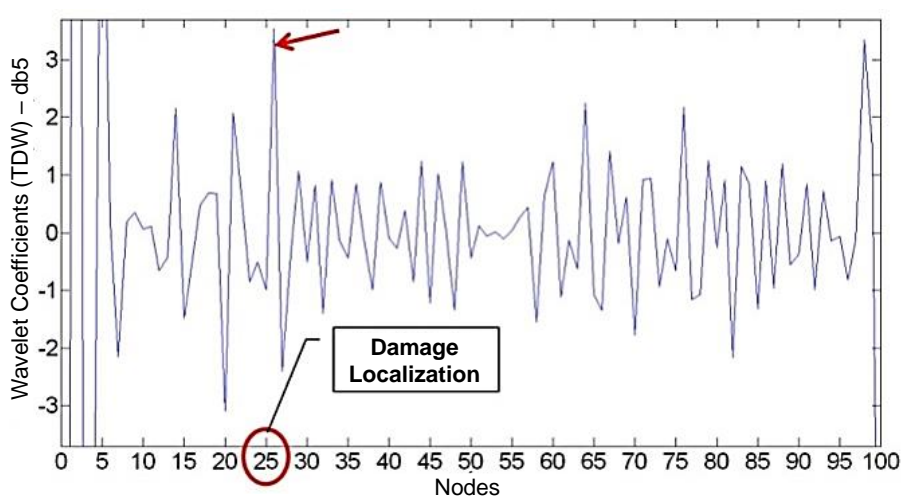


Figure 6 – DWT coefficients for V2E beam using db5.

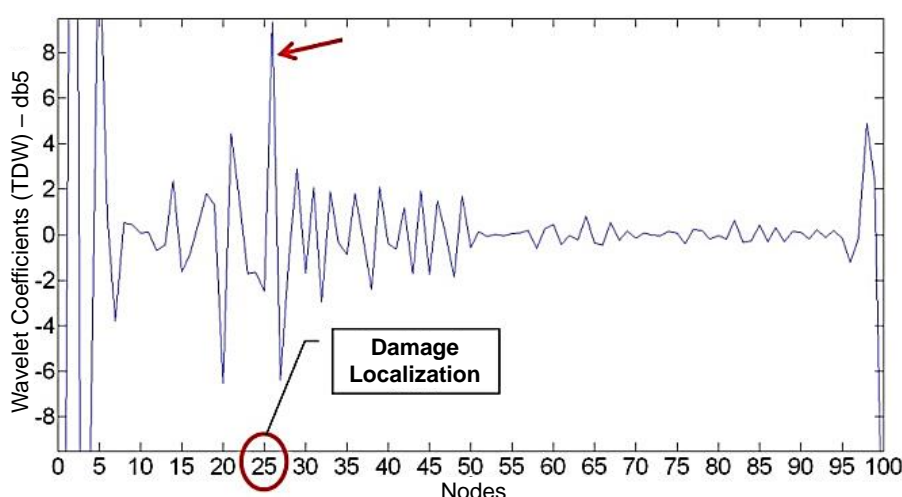


Figure 7 – DWT coefficients for V2E-2 beam using db5.

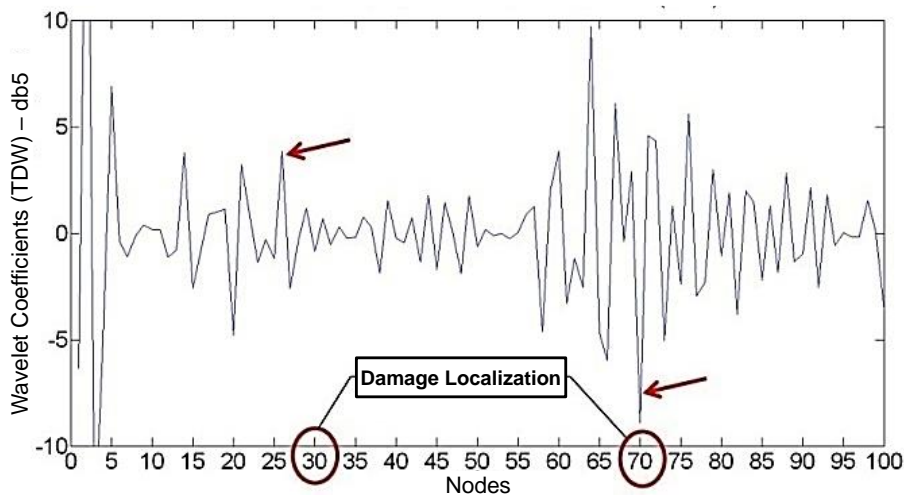


Figure 8 – DWT coefficients for V3E beam using db5.

### 3.2 Continuous wavelet transform results

Similar to DWT, Pachelor et al. (2014) select the same few set of mothers wavelets functions to calculate TDW coefficients of experimental data. Daubechies mother wavelet (db5) were choose due to others mother wavelets analyzed is similar. CWT presents the wavelet coefficients as function of position and scale which can be represented as 3D and 2D graph.

Figure 9 has the continuous wavelets coefficients of experimental static data of V2E beam using Daubechies mother wavelet (db5). Figure 10 and Figure 11 represent the same result for beam V2E-2 and V3E, respectively. The damage location using CWT is similar to DWT results. The damage is located at node 25 corresponding to 1.5 m from left support.

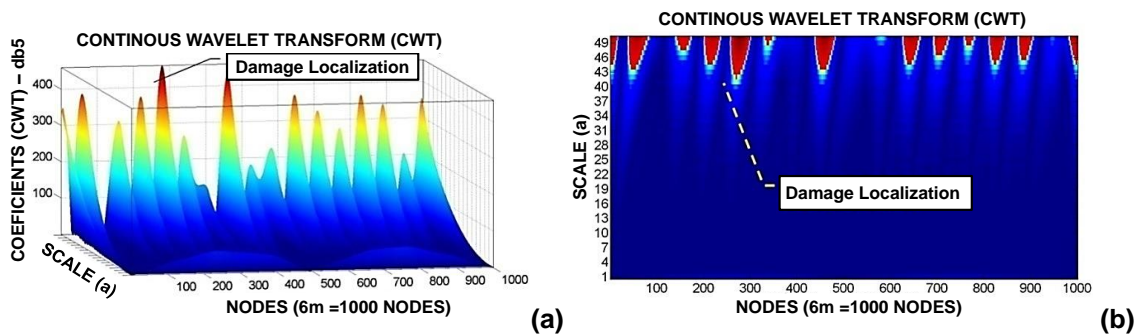


Figure 9 – CWT coefficients for beam V2E using db5: (a) 3D view and (b) 2D plan.

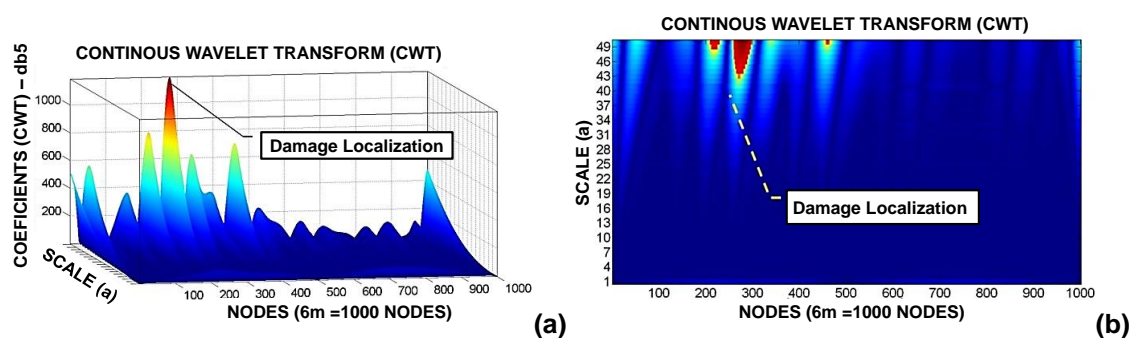


Figure 10 – CWT coefficients for beam V2E-2 using db5: (a) 3D view and (b) 2D plan.

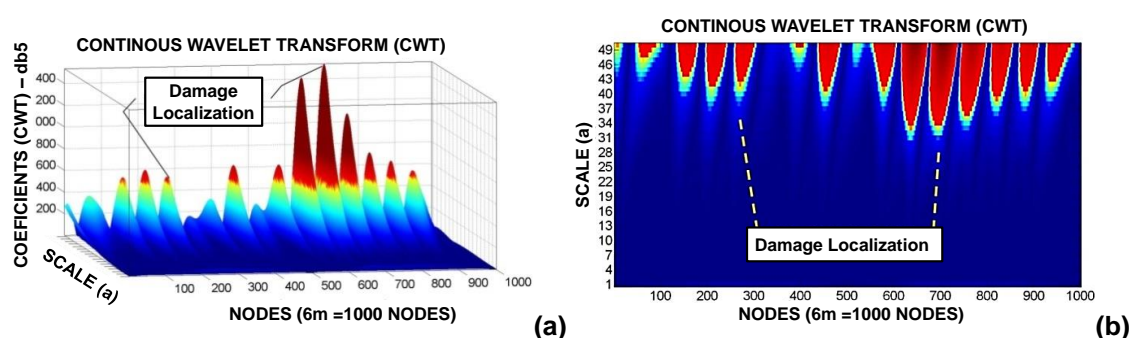


Figure 11 – CWT coefficients for beam V3E using db5: (a) 3D view and (b) 2D plan.

### 3.3 Important Remarks

We select some highlight:

- Continuous and discrete wavelet transform present similar results respect to damage localization
- The mother wavelet bior6.8, rbio2.6, sym6, coif3 and db5 are efficient to damage localization in experimented beams (Palechor *et al.*, 2014).
- Wavelet coefficients are sensitive to geometric discontinuities of structural supports. The wavelet coefficients graphs shown pics similar (or superior) to damage discontinuities.
- Wavelet coefficients are sensible to damage intensity. Intensity of damage results in wavelet coefficients picks. The open cracks with 4 cm cut present better results than 2cm cut.

## 4 Damage Detection in Bridge using Experimental Modal Shape

Silva et al. (2019) present a damage localization methodology using CWT associated with spline interpolation and regularization techniques applied to identified mode shapes. . As application test, the authors present the analysis of Dogna Bridge (Italy) using only damage response.

The villages of Crivela and Valdogna, located the Italian north east region, are connect by Dogna bridge crossing river Fella (Artemis Modal, 2014). This a reinforced concrete bridge has four-span with single-lane structure with 64m long (16m each) and 4m wide

(Figure 12ab). Three longitudinal beams, with rectangular cross-sections  $120 \times 35 \text{ cm}^2$ , support an 18cm-thick slab. Figure 12c shows transversal section of three longitudinal beams and slab. Progressive damage introduction is detailed in the next sections.

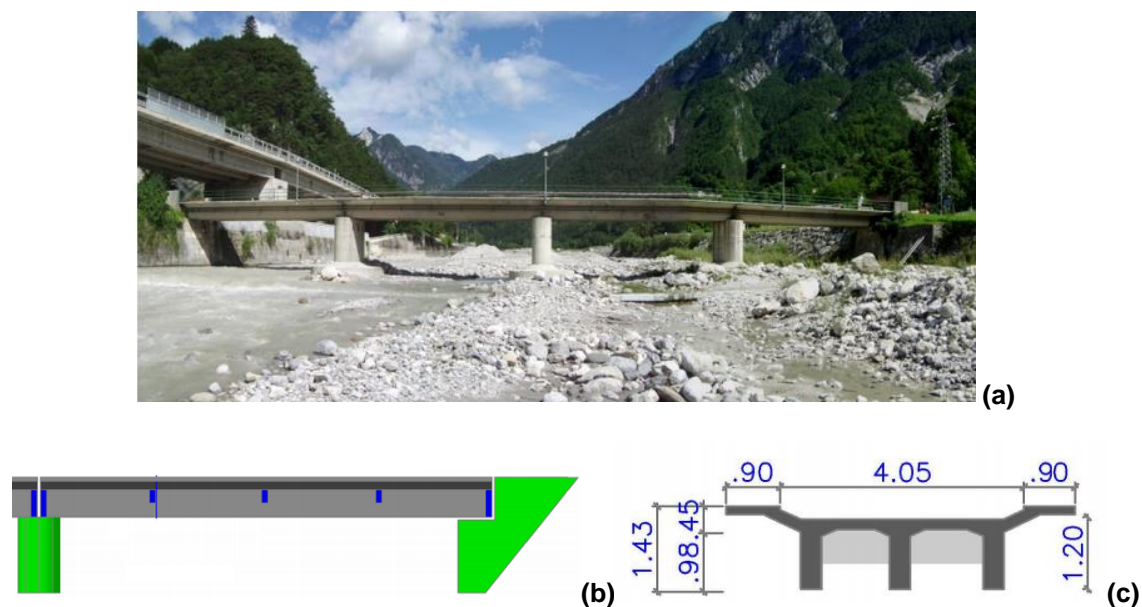


**Figure 12 – Picture with overview of Dogna Bridge (a) and its schematic representation of longitudinal view (b) and transversal section (c).**

#### 4.1 Proposed Methodology

The proposed methodology is based on the use of three well-known techniques: cubic spline interpolation, Tikhonov regularization (Friswell, 2007; Palechor *et al.*, 2022) and continuous wavelet Transform. Silva *et al.* (2019) applied the proposed methodology for damage localization using experimental data or numerical results.

Firstly, the data of damage structure need be obtained by experimental test or numerical simulation. And it is necessary extract the mode shapes from damage structure data. Secondly, the cubic spline interpolation determines intermediated spatial data due to experimental data are compose of few measurement points (Palechor, 2013). Thirdly, Tikhonov regularization technique reduce numerical oscillations of interpolated mode shape signal (Palechor *et al.*, 2022). Lastly, it is determined the continuous wavelet coefficients of regularized mode shape. It is search for discontinuities in wavelet coefficients plots that correspond to damaged region. Figure 13 summarize the flowchart of proposed methodology.

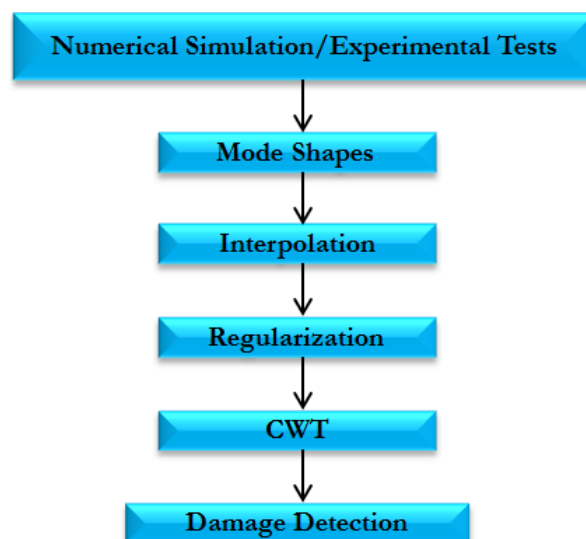


Figure 13 – Proposed methodology flowchart.

## 4.2 Dynamic test of intact bridge

The Dogna bridge was essayed experimentally to obtain the dynamic proprieties of modal frequency and modal shape. The dynamic test use ambient vibration, as excitation. Figure 14 show the position of ten accelerometers. All the experimental signal accelerations of intact and damaged bridge cases were provided by Structural Vibration and Solutions (SVIBS) company, developer of ARTeMIS software (Artemis Modal, 2022).

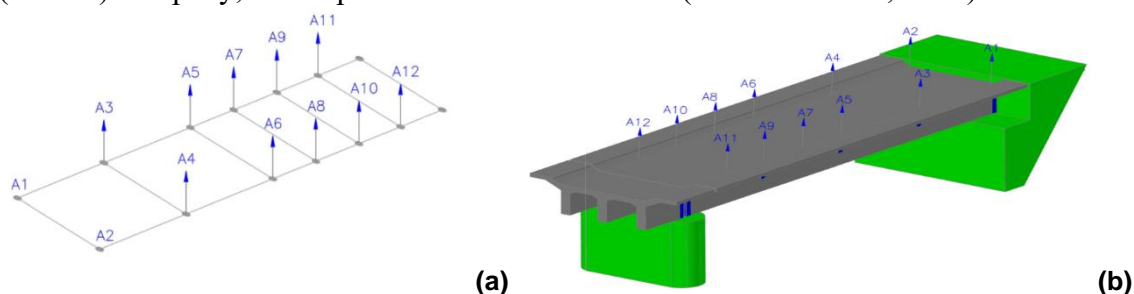


Figure 14 – Instrumentation in Dogna bridge:  
(a) instrumental layout and (b) perspective view.

The frequencies and mode shapes identification was performed using the frequency domain decomposition method available in ARTeMIS software (Artemis Modal, 2022). Numerical model of reinforced concrete bridge was done in Ansys Mechanical using element SOLID65 (3-D Reinforced Concrete Solid). The equivalent reinforced concrete material characteristics was modal elasticity  $E = 32GPa$ , Poisson ratio  $\nu = 0.3$  and concrete density  $\rho = 2500 kg/m^3$ . The degrees of freedom on the supports were modeled by imposing nodal displacement constraint at ends of longitudinal beams. Figure 15 to Figure 17 compare experimental and numerical of first three mode shape of undamaged bridge structure. Figure 18 show the average normalized singular values of spectral density functions of all experimental signal used by FDD technique. Figure 19 shows auto-MAC correlation matrix of experimental mode shapes with a good agreement of first three modal shapes.

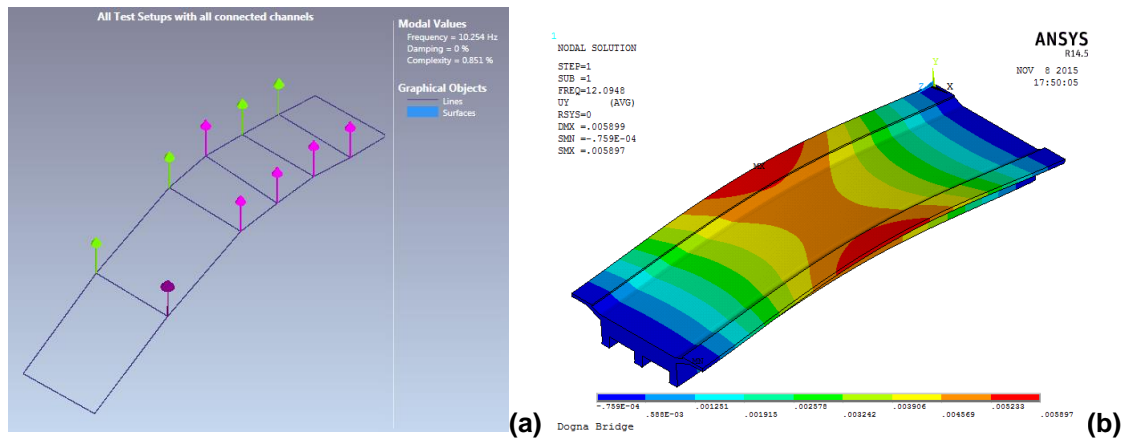


Figure 15 – First frequency mode shapes of intact beam: (a) experimental (10.25Hz), (b) numerical (12.09Hz).

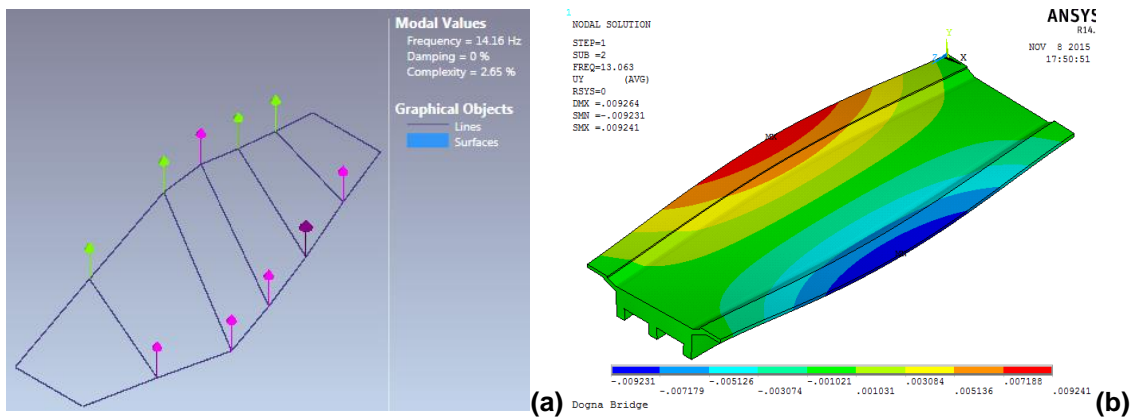


Figure 16 – Second frequency mode shapes of intact beam: (a) experimental (14.16Hz), (b) numerical (13.06Hz).

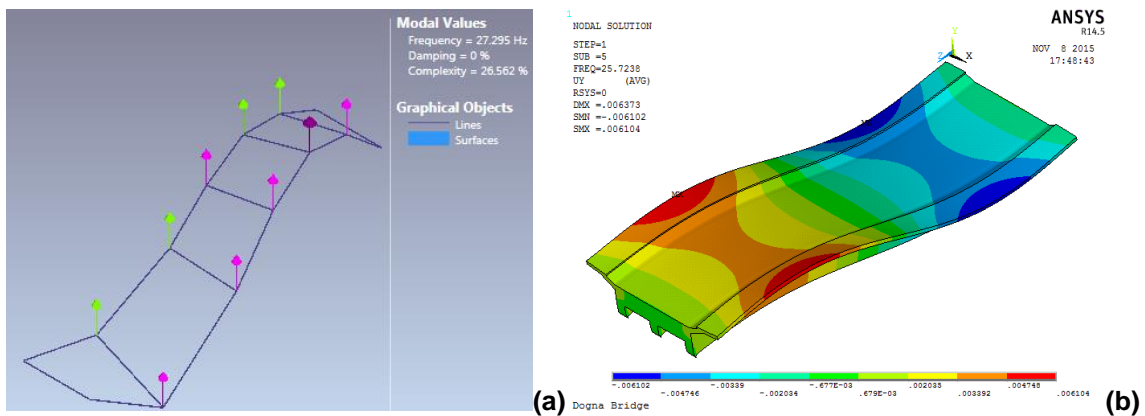


Figure 17 – Third frequency mode shapes of intact beam: (a) experimental (27.29Hz), (b) numerical (25.72Hz).

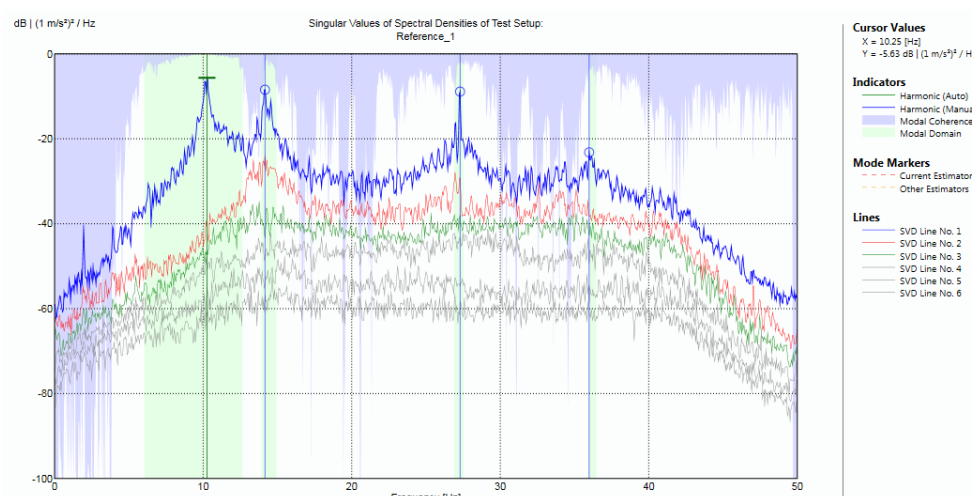


Figure 18 – Average normalized singular values of spectral density function using FDD.

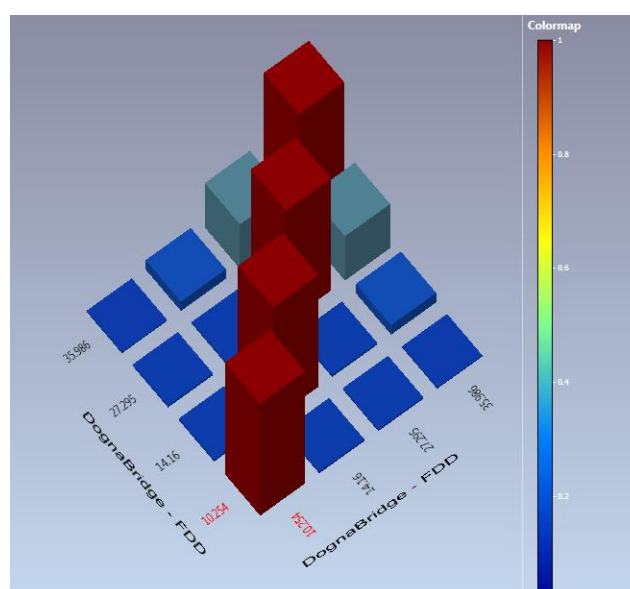
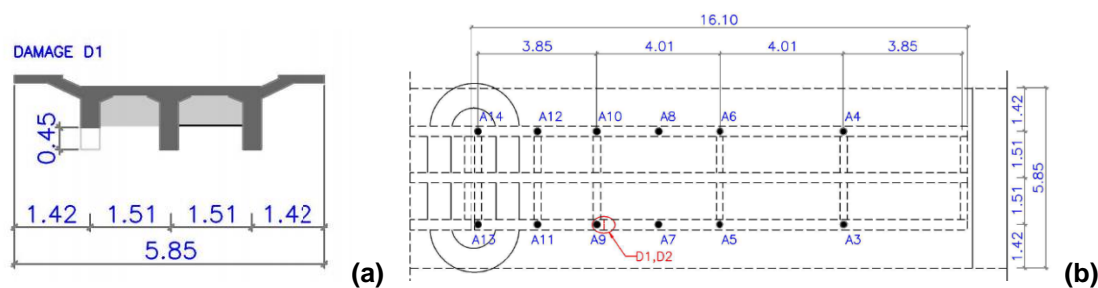


Figure 19 – AutoMAC correlation matrix of experimental mode shapes.

### 4.3 Damage localization

The damage case D1 consists of a half cut (45cm) of external beam. Damage case D1 represent reduction of 8% of total cross section of Dogna Bridge (Figure 20). A concrete cutter saw machine introduce the damage in external longitudinal beam (Figure 21). The experimental campaign for damage case D1 carries out a similar experimental procedure of intact case. Numerical modelling introduces damage deleting finite elements at the same position as the experimental test.



**Figure 20 – Transversal cut view of damage D1(a) and localization of damage position by plan view(b).**

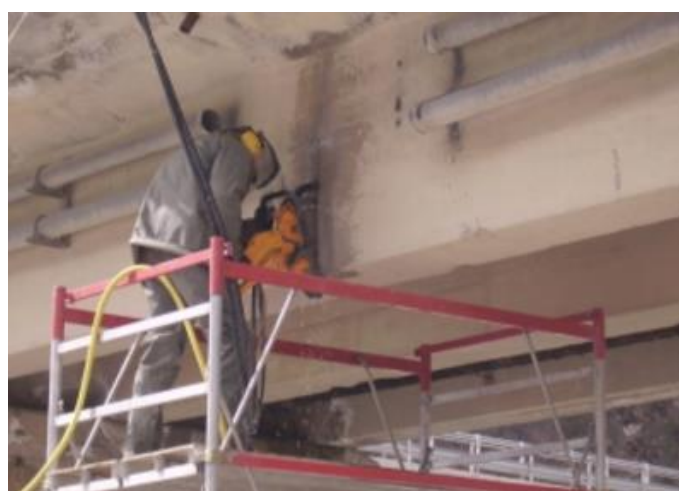


**Figure 21 – View of artificial introduction of damage in longitudinal beam.**

Table 4 compare modal frequency of first four modes for intact and damage D1 cases. presents the values of numerical natural frequencies of the intact and the damaged bridge. First frequency of experimental intact and damage results a sensible difference. And the numerical damage model presents a minor reduction compared to intact ones.

**Table 4 – Comparison of modal frequencies (Hz) for intact and damage case D1.**

Mode	Intact		Damage Case D1	
	Experimental	Numerical	Experimental	Numerical
1°	10.25	12.09	9.96	12.08
2°	14.16	13.06	14.06	13.05
3°	27.29	25.72	27.63	25.72
4°	35.99	38.29	35.32	38.28



Applying the proposed methodology, it's used the first mode shape of damaged D1 to determine damage localization. The data set of five points, corresponding to a line of first mode shape is exported to Matlab. Cubic spline interpolate this data set transforming 5 points in 1000 nodes. The Tikhonov regularization technique regularize this interpolated data set. Finally, CWT determine wavelet coefficients of regularized data set.

Figure 22 show the experimental and numerical comparison of CWT for damage D1 case. The determination of wavelet coefficients uses Daubechies5 wavelet mother function (Db5). We observe important discontinuity of wavelet coefficients near the damage position for experimental results and numerical model.

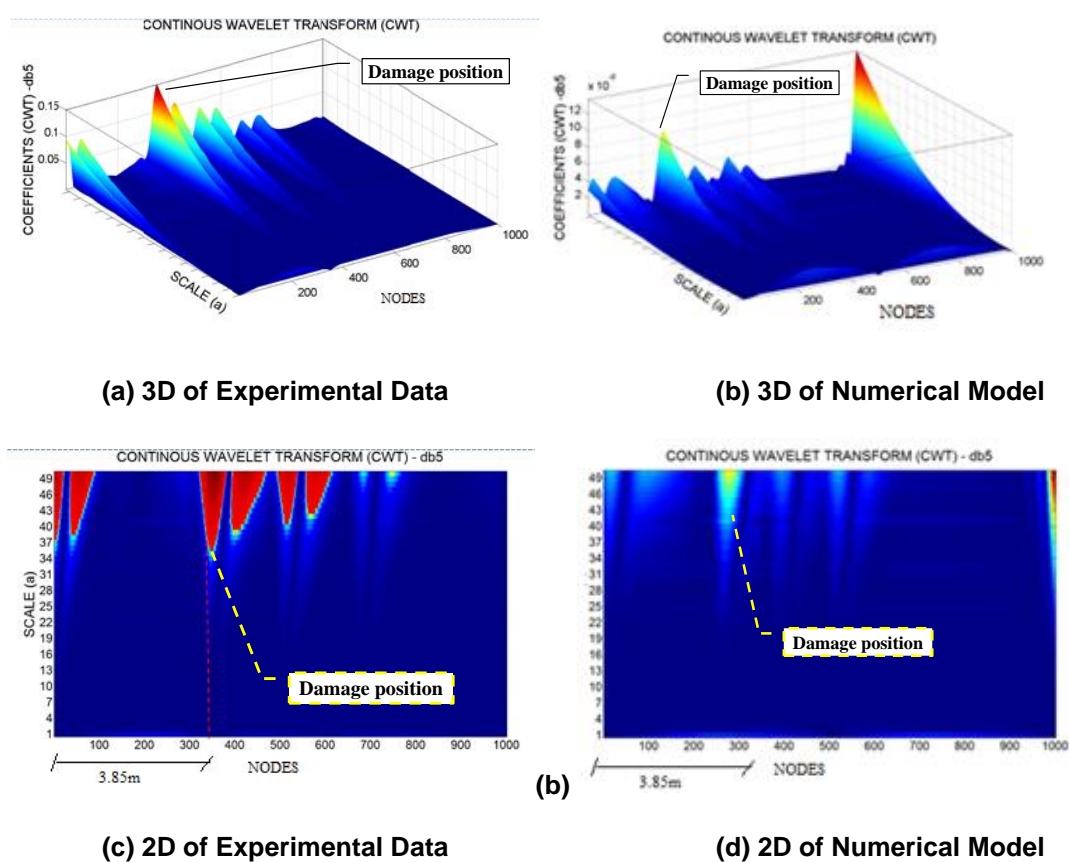


Figure 22 – Experimental and numerical comparison of CWT for damage D1 case.

### 5 Damage Detection using 2D Boundary Element Method

Silva, Bezerra et al (2019) localize damage in 2D structure by wavelet transform of static boundary element solution. After presenting boundary element formulation, we show some examples concerning the localization of subsurface cracks using static loads in two dimensional structures. Single and multi-cracks with different orientations inside two-dimensional structures with different support conditions are investigated. The results show the proposed numerical procedure is effective in indicating the location of damages.

## 5.1 Numerical examples

There are three cases of two-dimension deep beam: (a) cantilever beam single cracked, (b) cantilever beam single cracked with simulated noise, and (c) fixed panel multi-cracked. These three cases are simulated with same material with Young modulus  $E = 200\text{GPa}$  and Poisson ratio  $\nu = 0.30$ . The static solution, obtained by boundary element method, was carried out by internal points in reference line. DWT obtain wavelet coefficients using mother wavelet Biorthogonal 3.7 (bior3.7).

### 5.1.1 Cantilever beam

Figure 23 present a schematic representation of cantilever deep beam case with boundary conditions clamped-free, i.e., fixed in left side and free and right side. The dimensions are length  $L = 500\text{mm}$  and height  $H = 100\text{mm}$ . Static load is a concentrated force  $F = 500\text{kN}$  at the top of free right end. An embedded vertical crack with length  $25\text{mm}$ , are induced at a distance  $d = 330\text{mm}$ . Boundary element model discretized with 100 quadratic elements for beam domain and 25 quadratic elements for crack (Figure 23). Schematic representation illustrates reference line at  $25\text{mm}$  from bottom line, without intersect crack, with 480 discretized points equally distributed of  $1\text{mm}$ . The reference line starts at  $10\text{mm}$  away from left side and finish at  $10\text{mm}$  before right side. But previous analysis show that others reference line present similar results for wavelet transformation.

After simulate described BEM model using Elast\_qua (Silva, Bezerra, *et al.*, 2019), Figure 24 show beam deformed shape. Figure 25 show DWT wavelet coefficients of vertical displacement  $u(x)$ , from internal points of reference line, performed by MATLAB/Wavetoolbox Biorthogonal 3.7 (bior3.7).

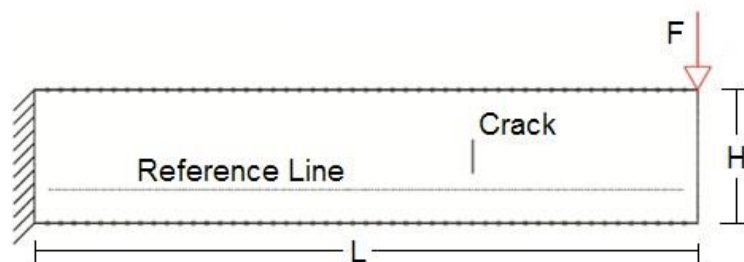


Figure 23 – BE mesh of cantilever beam case and internal nodes.

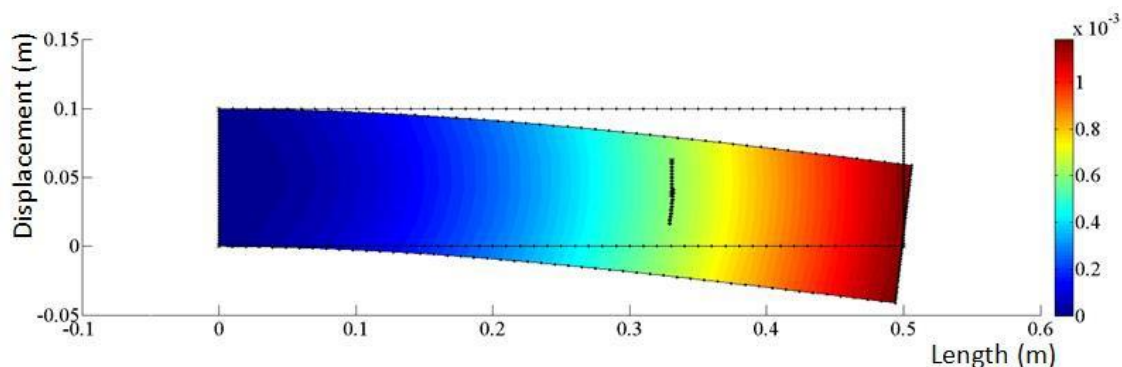


Figure 24 – Deformed shape of cantilever beam case.

Figure 25 shows wavelet coefficients results of DWT of  $u(t)$  (reference line). The position at 320 nodes correspond approximately to internal crack, i.e., estimated crack distance  $d_{est} = (320 - 1) \cdot 1mm + 10mm \approx 330mm$  is well estimated by present wavelet transformation. And similar to others results, it can be observed similar anomalous perturbation at extremity of wavelet coefficients DWT.

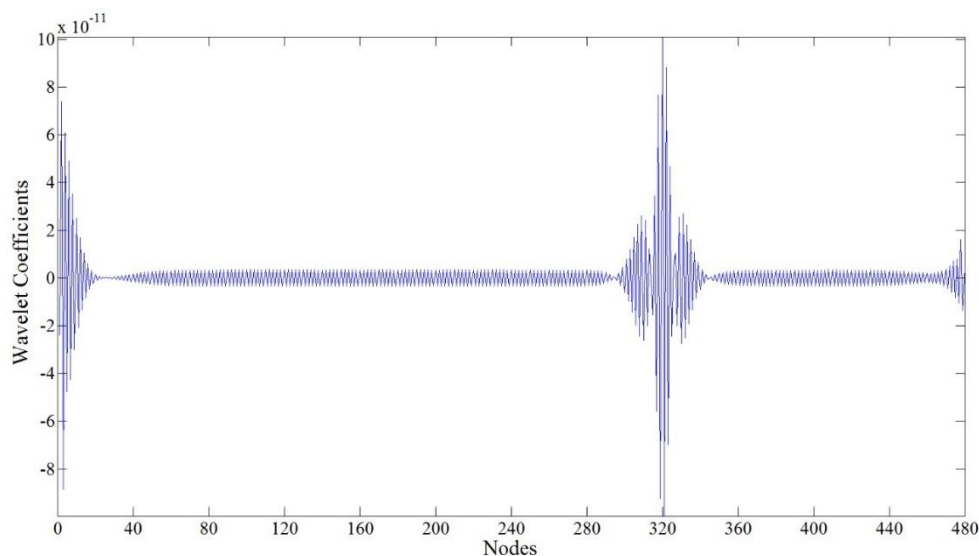


Figure 25 – Wavelet coefficients DWT using bior3.7 for cantilever beam case.

### 5.1.2 Cantilever beam with noise

During experimental tests, there are noticeable levels of noise in sensor readings signal. To simulate experimental conditions, white Gaussian noise has been introduced into static signal  $u(t)$  at reference line. The noise levels were 0.5%, 1% and 2% of noise of the maximum measured displacements.

As describe in Figure 26, the dimensions are length  $L = 500mm$  and height  $H = 100mm$ . And the concentrated load  $F = 500kN$  at top of free right side. An embedded vertical crack with length  $25mm$ , are induced at a distance  $d = 125mm$ . The reference line starts at  $10mm$  away from left side and finish at  $10mm$  before right side.

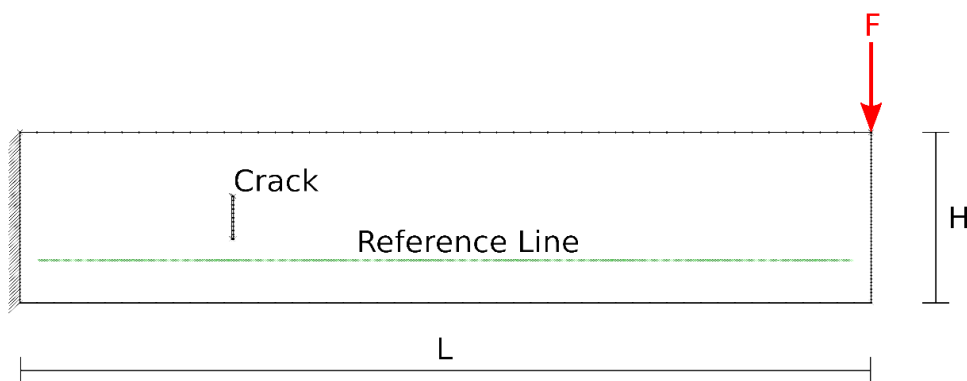


Figure 26 – BE mesh of cantilever beam case with noise.

Figure 27 show beam deformed shape. Figure 28 show DWT wavelet coefficients for the present cantilever beam without noise. Figure 29 to Figure 31 show DWT wavelet coefficients of static displacement  $u(t)$  added with 0.5%, 1.0% and 2.0% of white Gaussian noise, respectively. The noise/signal ratio is important to present methodology of damage localization. For low levels of noise, the disturbance in DWT wavelet coefficients do not difficult the localization of crack. But, with 2.0% of noise, the noise pollution difficult to detect clearly the crack position.

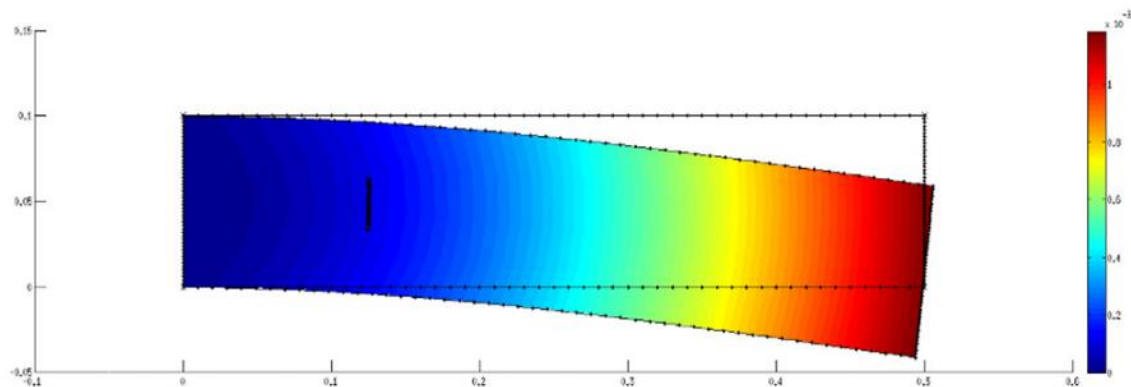


Figure 27 – Deformed shape of cantilever beam case with noise.

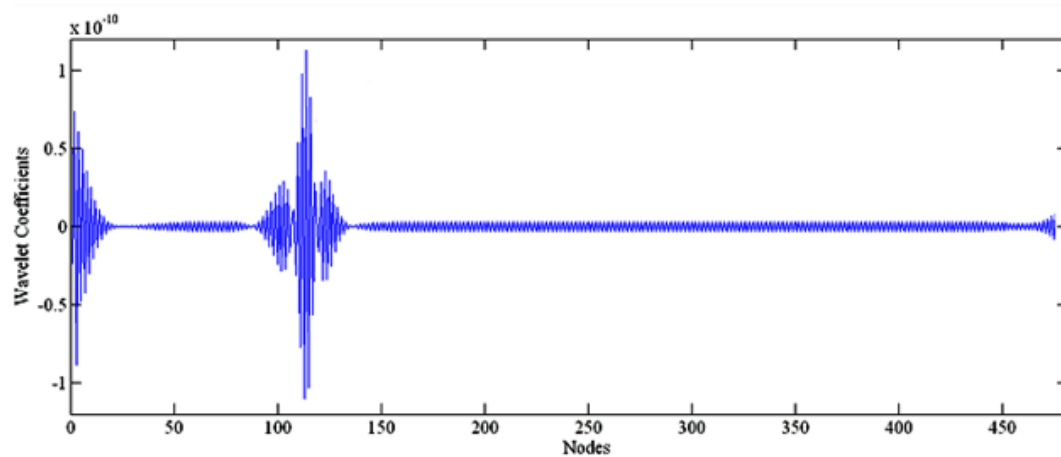


Figure 28 – Wavelet coefficients using bior3.7 of cantilever beam case without noise.

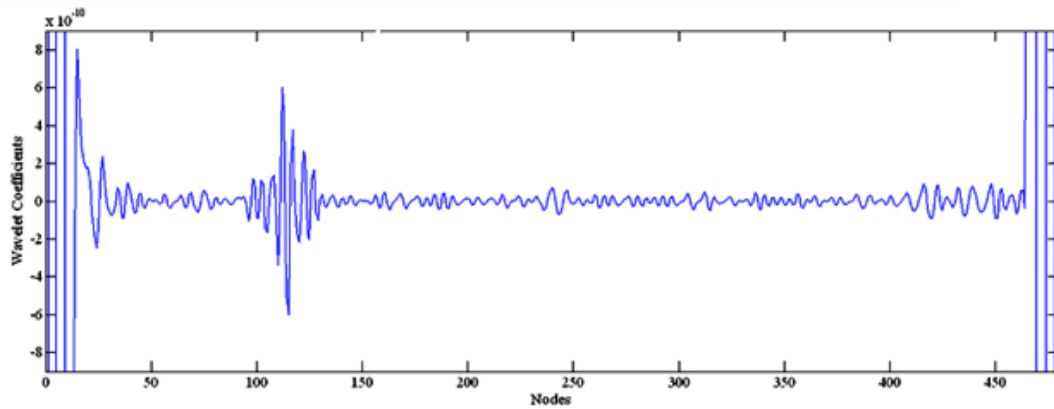


Figure 29 – Wavelet coefficients using bior3.7 of cantilever beam case with 0.5% of noise.

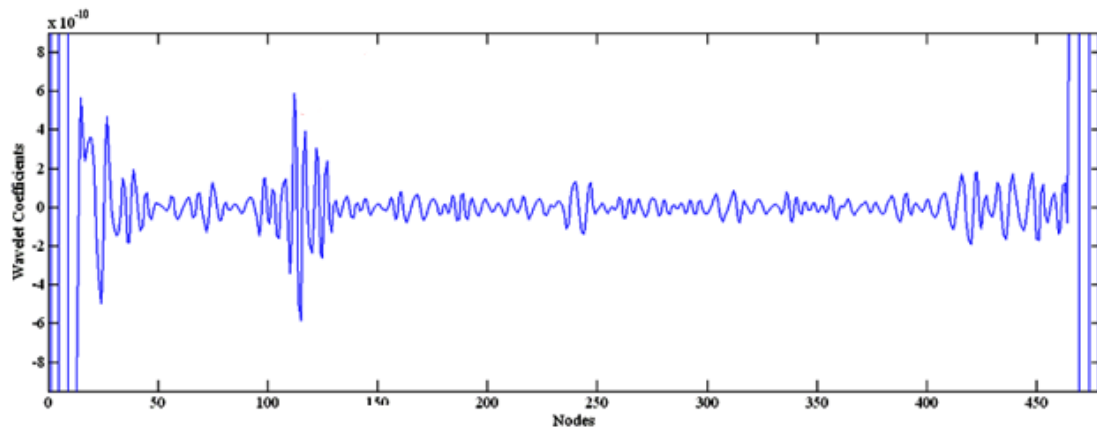


Figure 30 – Wavelet coefficients using bior3.7 of cantilever beam case with 1.0% of noise.

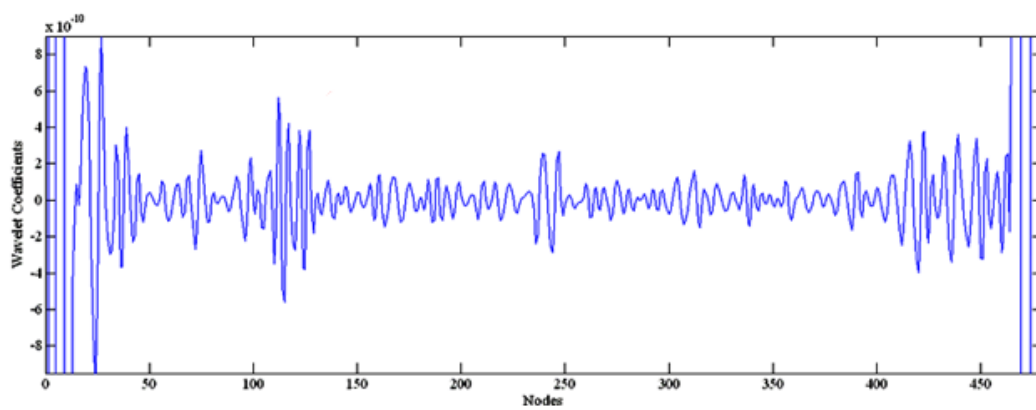


Figure 31 – Wavelet coefficients using bior3.7 of cantilever beam case with 2.0% of noise.

### 5.1.3 Beam with two fixed ends

Figure 32 show an example with coupled bending and tension forces. The panel fixed on left end. And a uniform distributed load  $q = 0.5kN/mm$  is applied vertically at panel top and horizontally at panel right end. The dimensions are length  $L = 2000mm$  and height  $H = 1000mm$ . Multiple cracks are positioned vertically ( $d = 333mm$  and  $1667mm$  at middle) and horizontally ( $d = 1000mm$ ) with respect left end side, as describe in Figure 32. Embedded cracks have length  $25mm$ . Reference line, positioned  $167mm$  from bottom line, is discretized with 480 nodes equally distributed. The reference line starts at  $44mm$  away from left side and finish at  $44mm$  before right side. Figure 33 show beam deformed shape.

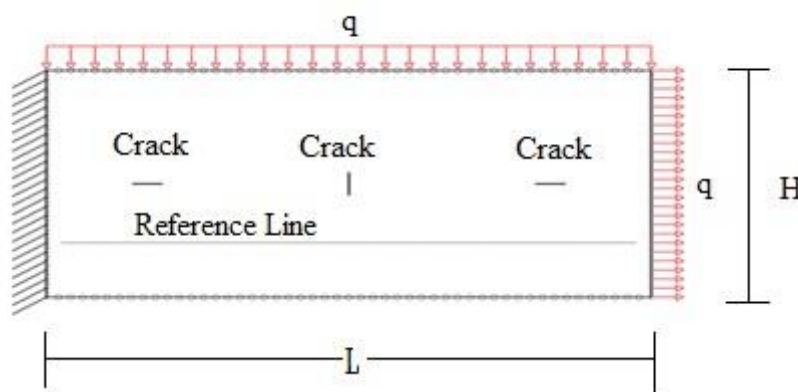


Figure 32 – BE mesh of panel with one side fixed.

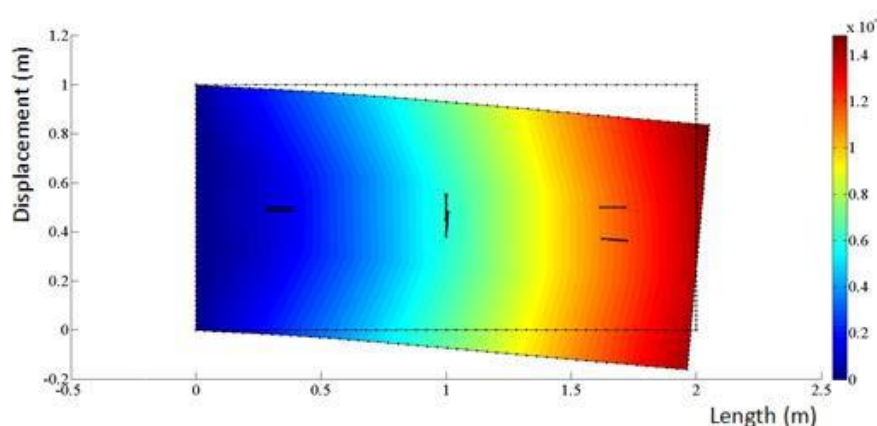
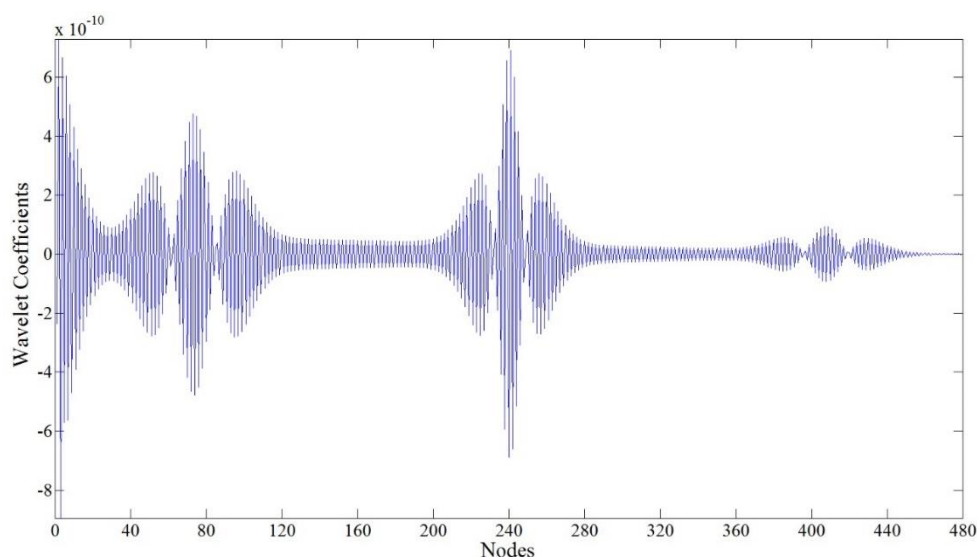


Figure 33 – Deformed shape of panel with one side fixed.

Figure 34 show DWT wavelet coefficients of vertical displacement  $u(x)$ , from internal points of reference line, performed by MATLAB/Wavetoolbox Biorthogonal 3.7 (bior3.7). The wavelet coefficients peaks correspond nodes 74, 240 and 408. These

peaks correspond to damages located with centers near to 339, 1000, and 1669mm measured from panel left end. Under coupled bending and tension forces, the bending deformation is more intense close to free end. The wavelet coefficients have narrow peaks near to vertical crack while the other horizontal cracks spread peaks in DWT. In any case, the numerical methodology was able to indicate the damage localization.



**Figure 34 – Wavelet coefficients DWT using bior3.7 of panel with one side fixed.**

## 6 Concluding remarks

Wavelet transform is an interesting tool to damage detection and localization. In this chapter, three research applications of wavelet transform are shown in 1D, 2D and 3D structures using experimental and/or numerical data. The wavelet transform only requires structure damage response. It's an advantage in comparison to traditional damage identification methods.

Firstly, the detection of open crack damage on laminated steel beams are presented using experimental static displacement. Discrete and continuous wavelet transform with Daubechies mother wavelets was applied to obtain wavelet coefficients of experimental data. Wavelet coefficients are sensible to damage intensity. The 40mm-depth cracks results in more intensive wavelet coefficients picks than 20mm-depth ones.

The second application presents the damage localization on Dogna bridge (Italy). Using a proposed methodology, a damage localization using continuous wavelet transform associated with spline interpolation and regularization techniques applied to experimentally identified mode shapes is presented. Numerical 3D FE model was calibrated with experimental data. The damage localization compares the wavelet coefficients of experimental data and numerical 3D FE results with similar results. As

application test, the authors present the analysis of Dogna Bridge (Italy) using only damage response.

At last, the wavelet coefficient was applied to localize damage in 3D structure modeled by boundary element method. Static response of elastic linear structures with single and multi-cracks was analysed using discrete wavelet transform. The damage localization using DWT with bi-orthogonal mother wavelets was effective. And noise/signal ratio is an important influence to methodology successfully.

## 7 References

- Artemis Modal (2014) *Damage Detection of the Dogna Bridge Italy, Internal Report*. Available at: <https://svibs.com/cases/damage-detection-of-the-dogna-bridge-italy/> (Accessed: 4 February 2022).
- Artemis Modal (2022) ‘Overview of ARTeMIS Modal Versions and Features ARTeMIS Modal is a powerful and versatile tool designed for the following analysis types: Operational Modal Analysis ( OMA ) Experimental Modal Analysis ( EMA ) Operating Deflection Shapes ( ODS ) Structura’, p. 2.
- Friswell, M. I. (2007) ‘Damage identification using inverse methods’, *Philosophical Transactions of the Royal Society A: Mathematical, Physical and Engineering Sciences*, 365(1851), pp. 393–410. doi: 10.1098/rsta.2006.1930.
- Janeliukstis, R. *et al.* (2017) ‘Experimental structural damage localization in beam structure using spatial continuous wavelet transform and mode shape curvature methods’, *Measurement*. Elsevier, 102, pp. 253–270. doi: 10.1016/j.measurement.2017.02.005.
- Kim, H. and Melhem, H. (2004) ‘Damage detection of structures by wavelet analysis’, *Engineering Structures*, 26(3), pp. 347–362. doi: 10.1016/j.engstruct.2003.10.008.
- Ovanesova, A. V. (2000) ‘Applications of Wavelets to Crack Detection in Frame Structures.’, p. 235.
- Ovanesova, A. V. and Suárez, L. E. (2004) ‘Applications of wavelet transforms to damage detection in frame structures’, *Engineering Structures*. Elsevier BV, 26(1), pp. 39–49. doi: 10.1016/j.engstruct.2003.08.009.
- Palechor, E. U. L. (2013) *Damage Identification in Steel Beams by Wavelets and Numerical/Experimental Signal (por. Identificação de Danos em Vigas Metálicas Utilizando Wavelets e Dados Numéricos e Experimentais)*. Universidade de Brasília. Available at: <https://repositorio.unb.br/handle/10482/14814>.
- Palechor, E. U. L. *et al.* (2014) ‘Damage Identification in Beams Using Experimental Data’, *Key Engineering Materials*, 607, pp. 21–29. doi: 10.4028/www.scientific.net/KEM.607.21.
- Palechor, E. U. L. *et al.* (2022) ‘Fundamental Concepts on Wavelet Transforms’, in.
- Silva, R. S. Y. R. C., Bezerra, L. M., *et al.* (2019) ‘Boundary element and wavelet transform methods for damage detection in 2D structures’, *International Journal for Computational Methods in Engineering Science and Mechanics*. Taylor & Francis, 20(3),



pp. 242–255. doi: 10.1080/15502287.2019.1631407.

Silva, R. S. Y. R. C., Palechor, E. U. L., *et al.* (2019) ‘Damage detection in a reinforced concrete bridge applying wavelet transform in experimental and numerical data’, *Frattura ed Integrità Strutturale*, 13(48), pp. 693–705. doi: 10.3221/IGF-ESIS.48.65.

Yang, C. and Oyadiji, S. O. (2017) ‘Damage detection using modal frequency curve and squared residual wavelet coefficients-based damage indicator’, *Mechanical Systems and Signal Processing*. Academic Press, 83, pp. 385–405. doi: 10.1016/j.ymsp.2016.06.021.